Minimum energy configurations of small bidisperse bubble clusters

2004 J. Phys.: Condens. Matter 16 4165

(http://iopscience.iop.org/0953-8984/16/23/031)

INSTITUTE OF PHYSICS PUBLISHING JOURNAL OF PHYSICS: CONDENSED MATTER

J. Phys.: Condens. Matter **16** (2004) 4165–4175 PII: S0953-8984(04)73778-9

Minimum energy configurations of small bidisperse bubble clusters

M F Vaz[1], S J Cox[2] and M D Alonso[2]

[1] ICEMS—Instituto de Ciência e Engenharia de Materiais e Superfícies, Departamento de Engenharia de Materiais, Instituto Superior Técnico, Avenida Rovisco Pais, Lisboa, Portugal
[2] Physics Department, Trinity College, Dublin 2, Republic of Ireland

E-mail: simon.cox@tcd.ie

Received 18 December 2003
Published 28 May 2004
Online at stacks.iop.org/JPhysCM/16/4165
DOI: 10.1088/0953-8984/16/23/031

Abstract

We consider two-dimensional foam clusters consisting of small collections of N bubbles with two different areas. Different arrangements of these bidisperse clusters were found experimentally for each N. Calculation of their perimeter allowed us to compare the energy of each cluster, giving candidates to the minimal energy arrangement. The number of possible clusters is discussed and the calculated energies are compared with existing approximations.

(Some figures in this article are in colour only in the electronic version)

1. Introduction

The determination of the minimum energy, or ground-state, of a two-dimensional (2D) foam with a given number of bubbles has recently attracted much attention. As well as the many practical applications of foams [1], for which a detailed knowledge of their structure is often important, such investigations provide a link between materials science and mathematics [2].

Impetus was given to the subject after Hales [3] proved the honeycomb conjecture: the minimum perimeter configuration of an infinite collection of equal-area cells is realized in the familiar hexagonal arrangement of the honeycomb. No such result exists for an infinite foam with bubbles of different areas.

A second approach is to consider finite collections of bubbles. The solution for a single bubble is well known, although the proof was less straightforward. For monodisperse (equal-area) clusters of N bubbles, exact solutions have been given for $N = 2$ (the double-bubble) by Foisy [4] and Morgan [5], and for $N = 3$ by Wichiramala [6]. For larger clusters, Vaz and Fortes [7] determined exactly the perimeter of the clusters formed by a central cell with n sides surrounded by one or two shells of six-sided cells. For more general monodisperse clusters, Vaz and Fortes [7] provide approximate formulae to estimate the perimeter. The

Surface Evolver program [8] was used by Cox and co-workers [9, 10] to provide candidate solutions for larger N (up to 10 000), showing that the minimal configuration is achieved when the shape of the cluster is 'facetted', with a hexagonal rather than circular shape determined by the influence of the hexagonal lattice underlying the bulk of the cluster. It is an open question as to how many possible clusters there are for each N, and therefore how many clusters should be tried before assuming that an optimal solution has been found.

Such 2D foams present an easily realized model of crystal structures, as exploited by Bragg and Nye [11]. Treating atoms as bubbles can thus give insight into atomic structure. In a related field, Manoharan *et al* [12] created 3D monodisperse clusters of colloidal microspheres that show intriguing patterns when they aggregate. The clusters appear to minimize the second moment of the mass distribution. Another analogy exists between wet foams and the packing of hard spheres. Stillinger *et al* [13] and O'Hern *et al* [14] studied the jamming behaviour of rigid discs and spheres. In our experiments, we were careful to allow the clusters freedom to explore fully the space of possible configurations and avoid such jamming.

1.1. Bidisperse clusters

The energy of a dry 2D foam is equal to the total length of the films multiplied by the film tension γ. In general, we wish to be able to predict the minimal energy and corresponding configuration of a cluster consisting of many bubbles with different areas. To make progress, however, we first study collections of bubbles with only two different areas. That is, for a cluster of N bubbles with two different areas A_i, we seek the configuration of bubbles giving the shortest perimeter.

Vaz *et al* [15] calculated precisely the total film length of a particular case of bidisperse clusters composed of a central cell surround by one or two shells of six-sided cells. They provide approximate equations for the energy of a general bidisperse 2D cluster. More recently Teixeira *et al* [16] determined analytically the minimum perimeter of finite *ordered* clusters with an equal number of regions with two different areas. Their candidates to each minimal cluster are of two types: large and small bubbles are either *mixed* or *sorted*. Their analysis applies only to clusters composed of more than 20 bubbles. The minimal configurations depend on the number of cells, N, and on the area ratio. For given N the minimal arrangement is of mixed type for large area ratios, while for smaller area ratios the bubbles are sorted. Similarly, small clusters tend to show mixing, but as N increases the minimal cluster is sorted, since the energy cost of formation of an interface decreases and favours sorted arrangements. Teixeira *et al* [16] did not compare their analysis with experimental data or the results of simulations.

In all this work, there is a lack of experimental data. Smith [17] introduced the experimental study of 2D free clusters of bubbles between glass plates, provoking a greater understanding of foams through an easily realizable system against which to test theory. In this case, it is not immediately clear that the *minimal* cluster will be found in an experiment, but by creating many configurations and then determining the energy of the most common ones computationally, we should have a high level of confidence in finding it, at least for small N.

For experimental simplicity, we further restrict ourselves to the study of bidisperse clusters of $N/2$ bubbles of area A_1 and $N/2$ bubbles of area A_2. We first prepared experimentally clusters with given N, A_1 and A_2. The candidates that appear most frequently in the experiments are expected to be the minimal ones. We therefore took these topologies and computed the energy of each of these clusters in the Surface Evolver.

We correlate the statistics on the frequency of experimental occurrence of a cluster with its energy to determine the effectiveness of our hypothesis that the minimal cluster is found most often. We then describe *shuffling* simulations, which enable us to estimate the number

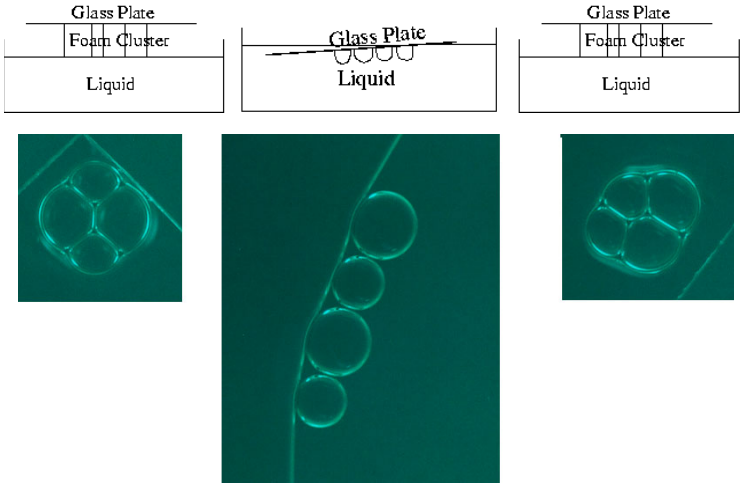

Figure 1. The experimental procedure consists of making a cluster of bubbles on the surface of a liquid and trapping them beneath a glass plate. The glass plate is then submerged and tilted, causing the bubbles to separate and allowing them to rearrange. The glass plate is then re-levelled to give a new cluster. The latter two steps (one *trial*) were repeated many times and the topology of each cluster was recorded.

of possible configurations for each N. Finally, we compare the energy given by the Surface Evolver with the predictions of Vaz *et al* [15].

2. Experimental procedure

A 2D bidisperse cluster is produced using a variant of the monolayer method [18, 19], previously used by Vaz and Fortes [7] to obtain 2D clusters of equal-volume bubbles. Air blown into a surfactant solution at *constant* pressure through a capillary tube forms small, equal-size bubbles. At high flow-rates there is an instability which means that although the bubbles are larger they are no longer monodisperse. In order to have two sizes of bubbles, we used two different size capillary tubes. The bubbles come to the surface of the surfactant solution and they are sandwiched between the liquid and a plexiglass plate above it. The gap between the plate and the surfactant solution was, with one exception, approximately $h = 3$ mm. In the case $N = 10$ we increased h slightly, which makes the cluster slightly drier. However, above a certain height there is an instability [20] in which two layers of bubbles are formed. The critical height at which this instability occurs varies with the volume and the number of sides of each bubble, so that we must keep h small to avoid two layers of bubbles being formed in any of the configurations.

When the bubbles are formed near each other they cluster together. We produced clusters with an even number of bubbles from $N = 4$ to 10, with half of the cells having each of the specified areas A_1 and A_2. Without loss of generality we assume $A_1 > A_2$.

The clusters are stable to small perturbations, such as shaking the container, but their topology can be changed by introducing large perturbations, such as tilting the plate on top of the cluster. We therefore explored different bubble configurations, for each N and area ratio, by tilting and re-levelling the plate, as shown in figure 1. Each of these *trials* allows the bubbles to rearrange in a new configuration: as we depress the plate the bubbles are pushed into the liquid and separate; re-levelling the plate will reassemble the bubbles [7] into a new cluster.

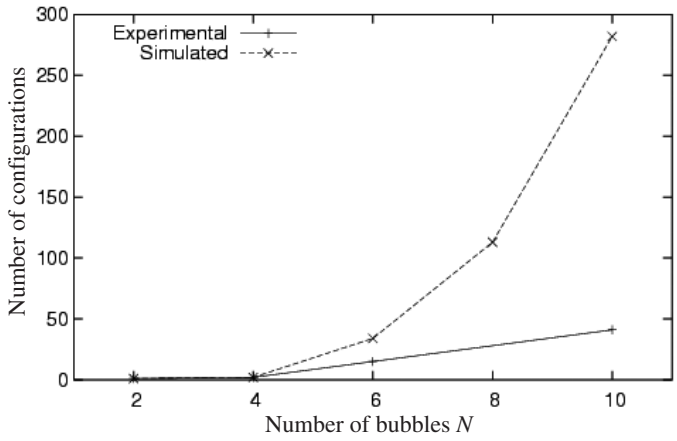

Figure 2. The number of observed clusters increases with the number of bubbles N. In the experiments this increase is approximately linear, while the simulations show that the total number of possible clusters increases much more rapidly: a power-law fit has an exponent close to 4 (actually 4.07 ± 0.122).

A large number of trials was performed for each N. In this way, several configurations were photographed, with bubble areas of 7, 14, 28, 38 and 50 mm^2 to give area ratios of 4/3, 2 and 4. These photographs were used for the subsequent analysis, described below. Submerging the cluster in the manner described above means that the topology of each cluster is not related to that of the previous one.

In some cases, the clusters were situated close to the edge of the plate. However, we obtained the same range of topologies away from the edges, suggesting that the proximity of the edge of the plate does not affect the topology of the cluster.

3. Observed clusters and frequency of occurrence

As the number of cells in the cluster increases, there is an increase in the number of observed configurations, shown in figure 2. For $N = 4$ we observed only two different arrangements, for $N = 6$ we found 15 different topologies and for $N = 10$ we obtained more than 40 configurations. For an asymmetric cluster we included both of the mirror images in the total, which means that we may underestimate the prevalence of symmetric clusters. We identify the clusters by the number of bubbles in the cluster and the ratio between the areas of the cells, $(N, A_1/A_2)$-j; the index j enumerates the different topologies found.

We focused our attention on clusters of four and six bubbles to study the effect of changing the relative size, A_1/A_2, of the bubble areas. We analysed the area ratios $A_1/A_2 = 4/3$, 2 and 4, performing 60 trials for each area ratio. Figures 3 and 4 show the observed topologies for 2D bidisperse clusters with $N = 4$ and 6 and $A_1/A_2 = 4/3$.

For $N = 10$ we fixed the area ratio at $A_1/A_2 = 2$ and varied the plate-separation h, with 160 trials at each of two different heights.

We determined the probability of occurrence of each topology. For $N = 4$, the lower energy cluster shown in figure 3(a) became more frequent as A_1/A_2 decreased. For $N = 6$, cluster 2 in figure 4 was the most frequent, followed by cluster 6. These flower-shaped clusters were found to be the minimal configurations for small monodisperse clusters [9] ($N = 6$, 7, 8) and it is therefore not surprising to see them here.

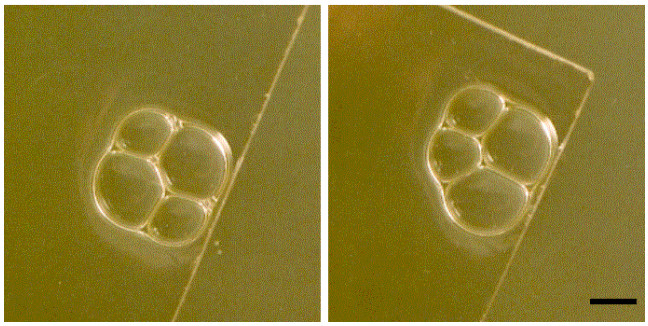

Figure 3. Observed clusters for four bubbles with an area ratio of 4/3. After 60 trials, two different topologies were observed: (a) (4, 4/3)-1 and (b) (4, 4/3)-2. (4, 4/3)-1 appeared least often, in only 33% of experiments. For other area ratios, (4, 2)-1 was observed in 43% and (4, 4)-1 in 54% of experiments. The reference line is 5 mm in length.

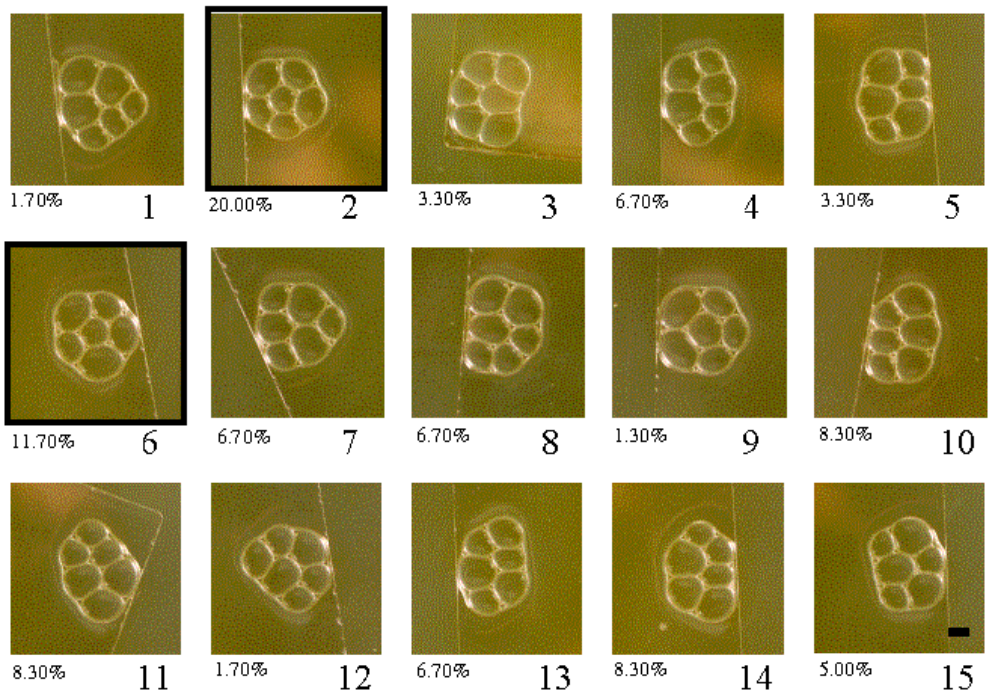

Figure 4. Observed clusters for six bubbles with an area ratio of 4/3, i.e. (6, 4/3)-j for j from 1 to 15, labelled with their frequencies of occurrence. Fifteen distinct topologies were found in 60 trials. For each area ratio configuration 2 appeared most frequently, followed by configuration 6. These are therefore the best candidates to the minimal configuration. The reference line shown for $j = 15$ is 5 mm in length.

The most frequent experimental cluster for $N = 10$ was the same for heights $h = 3$ and 3.5 mm. It is shown in figure 5(a); note that the bubbles are sorted by area.

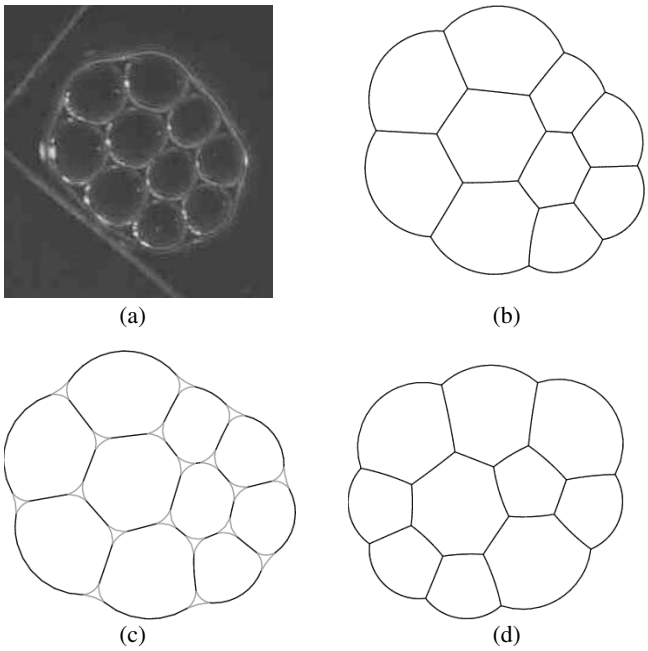

Figure 5. (a) A photograph of an experimental cluster of 10 bubbles with an area ratio of 2 and (b) the corresponding Surface Evolver image. This configuration was the most frequent after 320 experiments with two different plate separations. Note the large Plateau borders present in the experiment; these can be accommodated in the simulation, as shown in (c), but this does not result in a significant change to the *relative* energies of the different cluster configurations. (d) The lowest energy configuration among the forty experimental arrangements, calculated with the Surface Evolver.

4. Energy calculation

Our experiments have provided candidates to the minimum configuration in bidisperse clusters with different area ratios. We therefore reproduced each of the experimental configurations using the Surface Evolver [8] and determined its energy (line-length). Figure 5(a) shows a photograph of a cluster of ten bubbles and figure 5(b) the corresponding Surface Evolver image. We chose bubble areas of order one, since all choices are equivalent when the energy is scaled by $E/(\gamma\sqrt{\sum A_i})$. Further, we treat the gas inside the bubbles as incompressible and neglect local changes in the film tension.

The generation of clusters was based upon the dry model of a 2D foam in which the Plateau borders, which form at each triple junction of films, and their contribution to the energy are ignored. It is possible to include these borders, as illustrated in figure 5(c), by 'decorating' the vertices of the dry cluster with small triangles. The surface tension of each of the edges of these triangles is half the value of the existing films, since they consist of a single air–liquid interface. Notice that, since we assume that each of the borders has the same area, each border contributes the same extra length to the cluster's perimeter after the energy minimization process. Since each cluster of N bubbles has the same number, $2N - 2$, of Plateau borders, using this wet model of a 2D foam would result in the addition of the same constant to the energy of each cluster and would therefore not assist us in distinguishing clusters based upon their energy.

For $N = 4$ we find that the symmetric configuration in figure 3(a) has lower energy for each area ratio; not surprisingly, this is the minimal configuration. However, for $A_1/A_2 = 4/3$,

the difference between the lowest and the highest energy is less than 0.18%. This difference increases to 0.38% and 0.54% as the area ratio increases to 2 and 4 respectively. Thus only for the largest area ratio did our experiments show the minimal configuration most of the time.

For $N = 6$ the minimal cluster changes with the area ratio. For $A_1/A_2 = 4/3$ and 2 the minimal energy cluster is $j = 2$, but for $A_1/A_2 = 4$ the minimal energy arrangement is $j = 7$. The latter was not found most frequently in the experiments—this was configuration 2, as for the lower area ratios. As before, the values of energy are very close, although the differences increase with an increase in area ratio.

Calculations for $N = 10$ and $A_1/A_2 = 2$ showed that the lowest energy cluster is the one shown in figure 5(d). Its energy is 0.23% less than that of the cluster observed most frequently in the experiments. Although it only appeared once at a plate separation of $h = 3$ mm, with a drier cluster at $h = 3.5$ mm it was seen 15 times (almost as frequently as the configuration in figure 5(a)). Therefore as the cluster becomes drier, the correlation between frequency and energy improves.

The values of energy are compared with the frequency of occurrence of clusters $N = 6$ and 10 in figures 6(a) and (b) respectively. The data are rather scattered, but for each area ratio the best-fit straight line shows that the more frequently observed clusters have lower energy. The scatter suggests that our hypothesis that the lower energy clusters occur more frequently only holds on average, perhaps because the range of energies is small. The actual 3D nature of the experimental system, discussed below, must also have an effect.

We next seek to estimate the proportion of the possible configurations that were found in the experiments, to show how much of the 'phase-space' the experiments explore.

5. Shuffling simulations

It is unlikely that all possible clusters were observed experimentally for a given N, particularly as N increases. We therefore initiated a search using the Surface Evolver, with the aim of indicating the total number of possible clusters. In this search we discounted 'pathological' cases, such as N bubbles in a line, and started with two rows of $N/2$ bubbles. Our search thus estimates the number of 'rounded' clusters that could be expected to be found in the experiments, rather than answering the mathematical question of how many possible clusters exist.

We took a cluster of bubbles and performed various combinations of two shuffling steps:

- encouraging a topological T1 transformation on the shortest side in the cluster by deleting it, as described in [9];
- redistributing the bubble areas at random.

At each step the energy was recorded. The energy of each possible configuration was assumed to be unique, so that the number of different values of energy encountered reflected the number of clusters found in the shuffling process.

For values of $N = 6$, 8 and 10 we chose an area ratio of 2 and performed about 1000 shuffling steps. The lowest energy clusters are shown in figure 7, and the total number of clusters found in figure 2, which appears to increase with N^4 in contrast to the almost linear increase in the number of clusters observed experimentally.

For $N = 6$ we found a total of 34 configurations, twice as many as in the experiments. The procedure found all of the experimental configurations, and the lowest energy cluster is the one found in the experiment. For $N = 10$, the minimum energy arrangement in figure 7 was never observed experimentally. The difference in energy of the least-energy cluster found

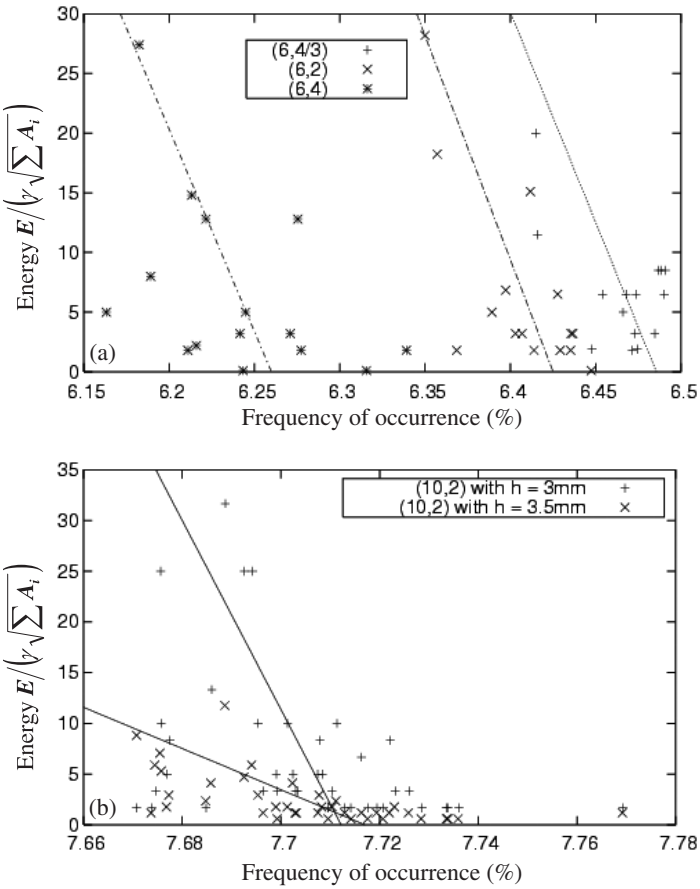

Figure 6. Frequency of occurrence of experimental clusters for (a) $N = 6$ and (b) $N = 10$ are compared to their calculated energies. The lines are linear fits, showing that on average the more frequently observed clusters have lower energies.

in the experiment (figure 5(d)) and the minimum energy one (figure 7) is 0.05%. For all values of N, the lowest energy cluster shows an axis of symmetry.

6. Approximate energy calculations

Graner *et al* [21] proposed an approximate equation for the energy E of a large 2D cluster of bubbles by neglecting the fraction of peripheral cells. For finite clusters, the contribution of the boundary must be considered [22], and Vaz *et al* [15] proposed the following equation to estimate the energy of a roughly circular 2D cluster:

$$\frac{E}{\gamma} = \frac{3.722}{2}\sum_i \sqrt{A_i} + 2.042\sqrt{\sum_i A_i}. \tag{1}$$

Those authors [15] also deduced a lower bound considering that in a cluster of regular hexagons of the same area with regular hexagonal boundary the factor 2.042 reduces to 1.934. Then the

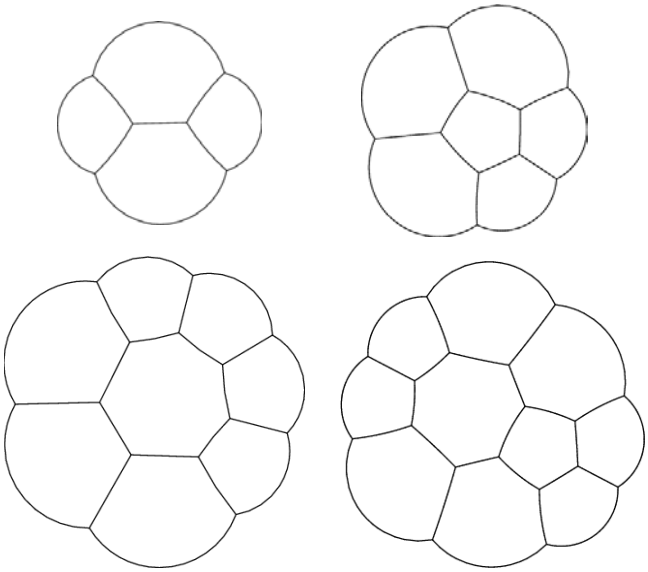

Figure 7. The lowest energy clusters found in the shuffling search with the Surface Evolver for each N with an area ratio of 2. Note that they are all symmetric, though not necessarily sorted, although in each case all the *large* bubbles touch.

lower bound for the energy can be calculated using

$$\left(\frac{E}{\gamma}\right)_{\text{l.b.}} = \frac{3.692}{2}\sum_i \sqrt{A_i} + 1.943\sqrt{\sum_i A_i}. \tag{2}$$

We have compared the energies obtained from the Surface Evolver, scaled according to $E/(\gamma\sqrt{\sum A_i})$, with equations (1) and (2), as a function of $\sum\sqrt{A_i}/\sqrt{\sum A_i}$. Figure 8 shows the Surface Evolver data for $N = 4$ and 6 with several area ratios ($A_1/A_2 = 4/3$, 2 and 4) and also for clusters of $N = 10$ bubbles with $A_1/A_2 = 2$. The lower bound shows broad agreement with the computations. Some values are, however, below the lower bound, which can be attributed to the small number of bubbles in our clusters.

Deviations from these equations were expected to increase with the width of the distribution of areas, i.e. at larger area ratios. This is because in approaching the monodisperse case, the differences in energies between different clusters with the same N are reduced, as is evident from the results for $N = 6$ shown in figure 8.

7. Summary

We have determined candidates to the minimal configuration for bidisperse clusters with a small number of bubbles. The high frequency of occurrence of certain topologies in the experiments gives an indication of the candidate configuration for each value of N and area ratio A_1/A_2. The calculation of the energy shows that, in general, the most frequently observed clusters tend to have lower energy. The correlation between experimental frequency and energy improves for drier clusters with larger bubbles. The values of energy obtained also exhibit good agreement with the equations derived by Vaz *et al* [15].

For very small N, it is not constructive to classify the minimal clusters as sorted or mixed. There appears to be a transition for $N = 6$ from sorted to mixed with increasing area ratio. This

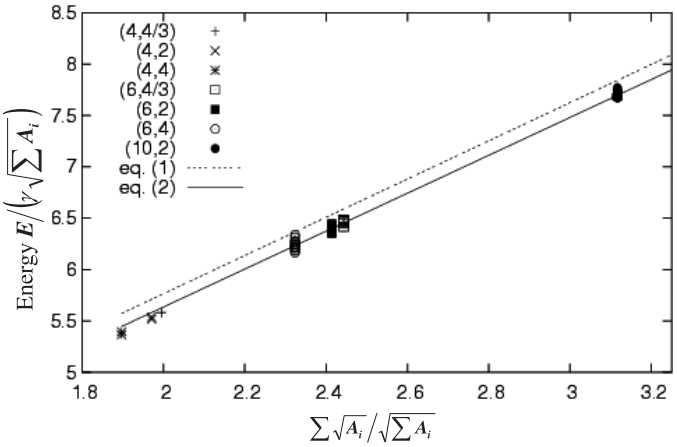

Figure 8. Energies obtained with the Surface Evolver (points) are compared with the approximations in equations (1) and (2) (broken lines). Although these analytic results show good general agreement with our results, for such small clusters the proposed lower bound is not appropriate since there are few, if any, bulk bubbles.

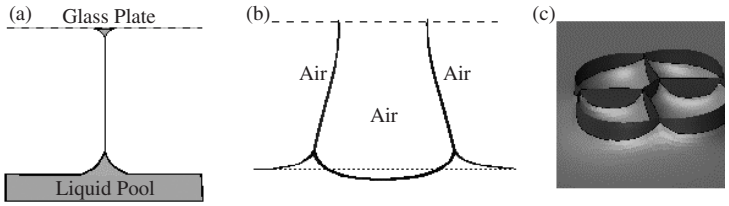

Figure 9. (a) Cross-section of the experimental set-up used for the experiments. The bubbles are trapped between a glass plate and the liquid surface. There is a Plateau border where the soap film meets the plate and a meniscus where the soap film contacts the liquid pool. (b) This image from a 3D Surface Evolver simulation shows the shape of the meniscus around a single bubble in this experimental system. Notice how it causes the bubble to deform: the bubble walls are no longer vertical and the bottom of the bubble is depressed below the still water level. The effect of the meniscus causes discrepancies between the 2D calculations and experiments. (c) A 3D calculation, such as the one shown here for the cluster (4, 4/3)-1, raises questions about the energy contribution of the meniscus; moreover, the vertical Plateau borders and those lying along the glass plate, which are not explicitly included in the calculation, must also play a role.

is in good agreement with the predictions of Teixeira *et al* [16]. For $N = 10$ the most frequent experimental cluster was sorted, but more striking is the *symmetry* of the Surface Evolver candidates to the minimum energy. While the number of clusters found in the experiment for each N increases approximately linearly, the *total* number of possible clusters increases with N^4.

Improved agreement between the frequency and energy data may be found by considering further contributions to the energy due to the actual 3D nature of the experimental system. In particular, the distribution of liquid in the meniscus and adjacent Plateau borders, illustrated in figure 9, gives corrections to the 3D surface energy. The quantification of these corrections is not a simple task, even though the meniscus can be incorporated into a 3D calculation as shown in figures 9(b) and (c). The *effect* of these contributions has been discussed by Cox *et al* [23]: the meniscus causes topological changes due to the attraction between neighbouring vertices. These topological changes can favour experimental configurations that have higher

'2D' energies. Thus shallow energy minima may be missed, even if they provide the global 2D minimum. On this basis, the better results obtained with a larger plate separation and larger bubbles are to be expected: the larger system size means that the relative size of the meniscus is reduced. We are currently exploring calculations of the energy of 3D systems such as this.

Acknowledgments

This work benefited from discussions with F Graner, M A Fortes, P Teixeira, D Weaire and I Cantat. MDA was supported by an IITAC fellowship and thanks IST for hospitality. SJC acknowledges financial support from the ELIPS programme of ESA.

References

[1] Weaire D and Hutzler S 1999 *The Physics of Foams* (Oxford: Clarendon)
[2] Taylor J 2002 *Bull. Am. Math. Soc.* **40** 69
[3] Hales T C 2001 *Discrete Comput. Geom.* **25** 1
[4] Foisy J, Alfaro M, Brock J, Hodges N, Zimba J and Morgan F 1993 *Pac. J. Math.* **159** 47
[5] *Geometric Measure Theory: A Beginner's Guide* 2000 (Boston, MA: Academic)
[6] Wichiramala W 2002 *PhD Thesis* University of Illinois
[7] Vaz M F and Fortes M A 2001 *J. Phys.: Condens. Matter* **13** 1395
[8] Brakke K 1992 *Exp. Math.* **1** 141
[9] Cox S J, Graner F, Vaz M F, Monnereau-Pittet C and Pittet N 2003 *Phil. Mag.* **83** 1393
[10] Cox S J and Graner F 2003 *Phil. Mag.* **83** 2537
[11] Bragg L and Nye J F 1947 *Proc. R. Soc.* A **190** 474
[12] Manoharan V N, Elsesser M T and Pine D J 2003 *Science* **301** 483
[13] Stillinger F, Sakai U and Torquato S 2003 *Phys. Rev.* E **67** 031107
[14] O'Hern C S, Langer S A, Liu A J and Nagel S R 2002 *Phys. Rev. Lett.* **88** 075507
[15] Vaz M F, Fortes M A and Graner F 2002 *Phil. Mag. Lett.* **82** 575
[16] Teixeira P I C, Graner F and Fortes M A 2002 *Eur. Phys. J.* E **9** 161
[17] Smith C S 1952 *Metal Interfaces* (Cleveland, OH: ASM) p 65
[18] Vaz M F and Fortes M A 1997 *J. Phys.: Condens. Matter* **9** 8921
[19] Rosa M E and Fortes M A 1998 *Europhys. Lett.* **41** 577
[20] Cox S J, Weaire D and Vaz M F 2002 *Eur. Phys. J.* E **7** 311
[21] Graner F, Jiang Y, Janiaud E and Flament C 2001 *Phys. Rev.* E **63** 11402
[22] Fortes M A and Rosa M E 2001 *J. Colloid Interface Sci.* **241** 205
[23] Cox S J, Vaz M F and Weaire D 2003 *Eur. Phys. J.* E **11** 29